

# Noncoding copy-number variations are associated with congenital limb malformation

Ricarda Flöttmann, MD<sup>1,2,\*</sup>, Bjørt K. Kragesteen, PhD<sup>1,2,\*</sup>, Sinje Geuer, PhD<sup>1</sup>, Magdalena Socha, PhD<sup>3</sup>, Lila Allou, PhD<sup>1</sup>, Anna Sowińska-Seidler, PhD<sup>3</sup>, Laure Bosquillon de Jarcy, MD<sup>2</sup>, Johannes Wagner, MD<sup>2</sup>, Aleksander Jamsheer, MD, PhD<sup>3</sup>, Barbara Oehl-Jaschkowitz, MD<sup>4</sup>, Lars Wittler<sup>1</sup>, Deepthi de Silva, MD<sup>5</sup>, Ingo Kurth, MD<sup>6,7</sup>, Idit Maya, MD<sup>8</sup>, Fernando Santos-Simarro, MD<sup>9,10</sup>, Wiebke Hülsemann, MD<sup>11</sup>, Eva Klopocki, PhD<sup>12</sup>, Roger Mountford, PhD<sup>13</sup>, Alan Fryer, MD<sup>13</sup>, Guntram Borck, MD, PhD<sup>14</sup>, Denise Horn, MD<sup>2</sup>, Pablo Lapunzina, MD<sup>9</sup>, Meredith Wilson, MD<sup>15</sup>, Bénédicte Mascrez, PhD<sup>16</sup>, Denis Duboule, PhD<sup>16,17</sup>, Stefan Mundlos, MD<sup>1,2</sup> and Malte Spielmann, MD<sup>1,18</sup>

**Purpose:** Copy-number variants (CNVs) are generally interpreted by linking the effects of gene dosage with phenotypes. The clinical interpretation of noncoding CNVs remains challenging. We investigated the percentage of disease-associated CNVs in patients with congenital limb malformations that affect noncoding *cis*-regulatory sequences versus genes sensitive to gene dosage effects.

**Methods:** We applied high-resolution copy-number analysis to 340 unrelated individuals with isolated limb malformation. To investigate novel candidate CNVs, we re-engineered human CNVs in mice using clustered regularly interspaced short palindromic repeats (CRISPR)-based genome editing.

**Results:** Of the individuals studied, 10% harbored CNVs segregating with the phenotype in the affected families. We identified 31 CNVs previously associated with congenital limb malformations and four novel candidate CNVs. Most of the

disease-associated CNVs (57%) affected the noncoding *cis*-regulatory genome, while only 43% included a known disease gene and were likely to result from gene dosage effects. In transgenic mice harboring four novel candidate CNVs, we observed altered gene expression in all cases, indicating that the CNVs had a regulatory effect either by changing the enhancer dosage or altering the topological associating domain architecture of the genome.

**Conclusion:** Our findings suggest that CNVs affecting noncoding regulatory elements are a major cause of congenital limb malformations.

*Genet Med* advance online publication 12 October 2017

**Key Words:** CNVs; congenital limb malformation; CRISPR-Cas9 genome editing; noncoding mutations; topological associating domains

## INTRODUCTION

The extensive clinical and genetic heterogeneity of congenital limb malformation requires comprehensive analysis of genome-wide genetic variation.<sup>1,2</sup> Microarray studies in single families have demonstrated the importance of copy-number variants (CNVs) in limb malformations, but until now no large scale-study in this context has been performed.<sup>3,4</sup> Recent advances in genome-wide DNA analysis technologies, such as array comparative genomic hybridization (CGH) and whole-genome sequencing, have led to an increased identification of

smaller noncoding CNVs.<sup>5–7</sup> Identified CNVs are generally interpreted by comparing them with existing databases, thus linking the effects of gene dosage with phenotypes. In many of these instances, however, these explanations are unsatisfactory; the effects of noncoding variants remain difficult to predict and many unexplained cases have been thought to result from so-called “position effects”.<sup>8,9</sup>

Our increased understanding of genomic folding has bolstered our ability to functionally annotate noncoding CNVs. Chromosome conformation capture (i.e., Hi-C) sequencing

<sup>1</sup>Max Planck Institute for Molecular Genetics, Berlin, Germany; <sup>2</sup>Institute for Medical Genetics and Human Genetics, Charité Universitätsmedizin Berlin, Berlin, Germany;

<sup>3</sup>Department of Medical Genetics, Poznan University of Medical Sciences, Poznan, Poland; <sup>4</sup>Gemeinschaftspraxis für Humangenetik Homburg/Saar, Homburg, Germany;

<sup>5</sup>Department of Physiology, Faculty of Medicine, University of Kelaniya, Ragama, Sri Lanka; <sup>6</sup>Institute of Human Genetics, Jena University Hospital, Friedrich-Schiller-University

Jena, Jena, Germany; <sup>7</sup>Institute of Human Genetics, RWTH Aachen, Aachen, Germany; <sup>8</sup>Raphael Recanati Genetics Institute, Rabin Medical Center, Beilinson Hospital, Petah Tikva,

Israel; <sup>9</sup>Instituto de Genética Médica y Molecular, IdiPAZ, Hospital Universitario La Paz, Madrid, Spain; <sup>10</sup>U753 Centro de Investigación Biomédica en Red de Enfermedades Raras,

Instituto de Salud Carlos III, Madrid, Spain; <sup>11</sup>Handchirurgie Kinderkrankenhaus Wilhelmstift, Hamburg, Germany; <sup>12</sup>Institute of Human Genetics, Biocentre, University of

Würzburg, Würzburg, Germany; <sup>13</sup>Merseyside and Cheshire Regional Molecular Genetics Laboratory, Liverpool Women's National Health Service Foundation Trust, Liverpool, UK;

<sup>14</sup>Institute of Human Genetics, University of Ulm, Ulm, Germany; <sup>15</sup>Department of Clinical Genetics, Children's Hospital at Westmead, and Disciplines of Paediatrics and Child

Health and Genetic Medicine, University of Sydney, New South Wales, Australia; <sup>16</sup>Department of Genetics and Evolution, University of Geneva, Geneva, Switzerland; <sup>17</sup>School of

Life Sciences, Federal Institute of Technology, Lausanne, Switzerland; <sup>18</sup>Department of Genome Sciences, University of Washington, Seattle, USA. Correspondence: Stefan Mundlos

(mundlos@molgen.mpg.de) or Malte Spielmann (spielman@uw.edu)

\*Ricarda Flöttmann and Bjørt K. Kragesteen contributed equally to this work.

Submitted 12 April 2017; accepted 11 July 2017; advance online publication 12 October 2017. doi:10.1038/gim.2017.154

experiments have revealed that the genome is divided into large, megabase-scale interacting compartments, termed A/B compartments, which are themselves composed of more local chromatin interaction units termed topological associating domains (TADs).<sup>10,11</sup> Neighboring TADs are separated by boundary regions that are strongly enriched in architectural proteins (i.e., CTCF and cohesion).<sup>12</sup>

The discovery of TADs and our increased understanding of long-range regulation have allowed us to better understand the mechanisms underlying position effects.<sup>10</sup> CNVs have the potential to alter the architecture of TADs within the genome by deleting or duplicating noncoding enhancer elements, or misplacing TAD boundaries.<sup>3,7,13,14</sup> These findings are directly relevant to human genetics, especially considering that most genetic studies focusing on coding variants failed to identify the molecular cause in over 40% of the families studied.<sup>15,16</sup> A large proportion of the remaining cases may therefore be explained by alterations outside the coding regions.

In this study, we performed copy-number analysis in 340 unrelated individuals with congenital limb malformation. In 10% of the families, we identified CNVs that were either *de novo* or segregated with the phenotype in the affected families. To further investigate four novel candidate CNVs, we generated transgenic mice using the clustered regularly interspaced short palindromic repeats (CRISPR)–CRISPR associated protein 9 (Cas9) system. Our data indicate that most CNVs in this cohort of patients with congenital limb malformation affect noncoding regulatory elements.

## MATERIALS AND METHODS

### Subjects and ethics approval

Venous blood and genomic DNA samples were obtained from the subjects using standard procedures. All individuals provided written informed consent to participate in the study and have their patient photos published. The study was approved by the Charité Universitätsmedizin Berlin ethics committee.

### Microarray-based CGH

Array CGH was carried out using a whole-genome 1 M oligonucleotide array (Agilent; Santa Clara, CA). 1 M arrays were analyzed by Feature Extraction version 9.5.3.1 and CGH Analytics version 3.4.40 or Cytogenomics version 2.5.8.11 software, respectively (Agilent). The analysis settings used were as follows: aberration algorithm: ADM-2; threshold: 6.0; window size: 0.2 Mb; filter: 5probes, log<sub>2</sub> ratio = 0.29. Data were submitted to the Database of Chromosomal Imbalance and Phenotype in Humans using Ensembl Resources (DECIPHER; <http://decipher.sanger.ac.uk>); accession numbers are listed in **Supplementary Tables S3–5**.

### Quantitative real-time polymerase chain reaction (qPCR)

We performed qPCR as previously described<sup>17</sup> using genomic DNA of the index subjects and family members to confirm the deletions and show segregation with the phenotype. The primer sequences are given in **Supplementary Table S6**.

### CRISPR single-guide RNA selection and cloning

Single-guide RNA was designed flanking the regions to be rearranged. We used the <http://crispr.mit.edu/> platform to obtain candidate single-guide RNA sequences. Complementary strands were annealed, phosphorylated, and cloned into the BbsI site of the pX459 or pX330 CRISPR–Cas vector. The CRISPR single-guide RNA sequences are listed in **Supplementary Table S7**.

### Mouse strains

The *Del(rel5-Atf2)* allele is described by Montavon *et al.*<sup>18</sup> The transgenic mice were generated from G4 cells (129xC57BL/6 F1 hybrid embryonic stem cells). The calculation of sample size was performed by power analysis and randomization was performed. The investigator was blinded to the group allocation of the animals during the experiment.

### Generation of transgenic embryonic stem cells

Roughly 300,000 G4 cells (129xC57BL/6 F1 hybrid embryonic stem cells) were seeded on CD-1 feeders and transfected with 8 µg of each CRISPR construct using FuGENE technology (Promega; Madison, WI). When the construct originated from the pX330 vector, cells were cotransfected with a puromycin-resistant plasmid. In contrast, PX459 already contains a puromycin-resistant cassette. After 24 h, the cells were split and transferred onto DR4 puromycin-resistant feeders and selected with puromycin for 2 days. Clones were then grown for 5–6 more days, picked and transferred into 96 well plates on CD-1 feeders. After 2 days of culture, the plates were split in triplicates—two for freezing and one for growth and DNA harvesting. Positive clones identified by PCR or Sanger sequencing were thawed and grown on CD-1 feeders until they reached an average of 4 million cells. Three vials were frozen and DNA was harvested from the rest of the cells to confirm genotyping. PCR-based genotyping and qPCR were performed as previously described.<sup>17</sup>

### Embryonic stem cell aggregation

A frozen embryonic stem cell vial was seeded on CD-1 feeders and cells were grown for 2 days. Mice were generated by morula aggregation and tetraploid complementation.<sup>19</sup> All animal procedures were in accordance with institutional, state, and government regulations (Landesamt für Gesundheit und Soziales, Berlin, Germany).

### In situ hybridization and skeletal preparations

In situ hybridization for *Fgf8* and *Nkx2–3* was carried out on wild-type embryos (C57/Bl6J) and mutant embryos at embryonic stage E11.5. Skeletal preparations and alizarin red staining of E18.5 wild-type and mutant embryos was performed as previously described.<sup>20</sup>

### Databases and in silico analysis

We used the databases DECIPHER (<https://decipher.sanger.ac.uk/>), ClinVar (<http://www.ncbi.nlm.nih.gov/clinvar/>), and the Database of Genomic Variants (<http://dgv.tcag.ca/dgv/>)

app/home), and the VISTA Enhancer Browser (<http://enhancer.lbl.gov>) to classify the CNVs.<sup>21–23</sup> The processing of the Hi-C data was performed by the Ren Lab<sup>10</sup> and downloaded via <http://chromosome.sdsc.edu/mouse/hi-c/download.html>.

The Gene Expression Omnibus accession numbers for the chromatin immunoprecipitation followed by high-throughput DNA sequencing data for the H3K27ac enhancer mark reported by Cotney *et al.* are GSE42413 and GSE42237.<sup>24</sup>

## RESULTS

We collected a cohort of 340 individuals affected with isolated congenital limb malformations. After clinical and radiographic examination, we performed high-resolution array CGH as a first screening test (**Figure 1** and **Supplementary Table S1**). Segregation analysis in the parents was performed by qPCR after comparing candidate CNVs with known limb genes according to the Human Phenotype Ontology project,<sup>25</sup> cross-species phenotype comparison,<sup>26</sup> mouse models,<sup>27</sup> gene expression data,<sup>28</sup> limb enhancer elements,<sup>24,29,30</sup> and the TAD architecture of the locus.<sup>10,16</sup> The results are summarized in **Supplementary Tables S2–5**. We detected 715 CNVs (>10 kb) that were extremely rare or absent in the common CNV databases (Supplementary Information). We identified 35 CNVs in unrelated individuals that were de novo or segregating with the phenotype in the family, corresponding to 10% in this cohort. A total of 31 subjects harbored CNVs that had previously been linked to disease in at least three unrelated individuals (**Supplementary Figure S1** and **Supplementary Tables S3–5**, including literature references). In addition, we identified CNVs in four regions that had not previously been linked to limb malformations (**Supplementary Table S2**).

Next, we investigated how many cases could be explained by gene dosage (gain or loss) of a known disease gene located within the CNV, and how many CNVs did not include a disease gene themselves, but might result from a noncoding position effect on neighboring genes. We manually inspected the entire TAD around each CNV for the presence of the following features: genes known to play a role in limb development or limb genes according to the Human Phenotype Ontology (HPO),<sup>25</sup> cross-species phenotype data,<sup>26</sup> available mouse models,<sup>27</sup> or available gene expression data.<sup>28</sup> We also screened the regions inside and around each CNV for the presence of known enhancers that might drive expression in the limb according to the VISTA database<sup>23</sup> and based on chromatin immunoprecipitation sequencing experiments performed in human and mouse limb tissues.<sup>24,29,30</sup> In addition, each CNV was placed within known Hi-C maps of the human genome to investigate its position relative to TADs and their boundaries.<sup>10,31</sup>

### Disease-associated loci: gene dosage

In 15 of the 35 subjects (43%), we identified CNVs that had previously been associated with disease in at least three unrelated individuals (**Supplementary Table S3**). Five

showed de novo deletions of genes known to be involved in limb defects based on reported cases with de novo loss-of-function mutations (**Supplementary Figure S2**) (i.e., *DLX5/DLX6*, *GDF5*, *GLI3*, *HDAC4*, and *ZAK*). Five subjects carried de novo tandem duplications of *BHLHA9*, a known cause for split hand/foot malformation.<sup>32</sup> The exact pathomechanism of *BHLHA9* duplications is still unclear, but the gene is highly expressed in the apical ectodermal ridge, and homozygous mutations in *BHLHA9* cause syndactyly.<sup>32,33</sup>

In five subjects, we identified recurrent microdeletion or microduplication syndromes (i.e., 16p11.2 microdeletion syndrome, 16p13.1 microduplication syndrome, or 2q37.3 microdeletion syndrome). These microdeletion or microduplication syndromes are characterized by a highly variable phenotypic spectrum and low penetrance. While limb defects have been described in patients with these recurrent CNVs,<sup>34</sup> it is likely that other modifiers also contribute to the limb defects.

### Disease-associated loci: noncoding *cis*-regulatory effects

In 16 of the 35 individuals (46%), we identified CNVs that had previously been associated with limb defects in at least three unrelated individuals. These CNVs did not include a disease gene themselves, but resulted in a position effect on known limb genes (**Supplementary Table S4**). Three of the subjects carried de novo CNVs deleting an enhancer element resulting in a tissue-specific loss of function of the limb genes *DLX5/6* over 950 kb telomeric to the deletion. Eleven subjects harbored duplications of limb enhancer elements causing a regulatory gain of function of the known disease genes *SHH* and *FGF8*. The duplicated enhancer elements were located 1 Mb and 200 kb away from their target genes, respectively. Two subjects had CNVs resulting in “enhancer-adoption” at the *PAX3* locus. This mutational mechanism describes the disruption of a TAD boundary, thereby allowing enhancers from neighboring domains to ectopically activate genes to cause misexpression and consequently disease.<sup>14</sup>

### Novel candidate loci

In 4 of the 35 individuals (11%), we identified CNVs at loci previously not known to be associated with limb malformations (**Figure 2a–d** and **Supplementary Table S2**). Three CNVs were de novo and one segregated perfectly with the phenotype in a large family. To investigate these candidate CNVs, we took advantage of an existing mouse model at the *HoxD* locus<sup>18</sup> and re-engineered the other human CNVs in mice using the CRISPR–Cas9 system. We used two guide RNAs in mouse embryonic stem cells to generate large deletions and duplications.<sup>17</sup>

We detected a 440-kb microdeletion on chromosome 2q31 in an individual with shortening of the metacarpals compatible with a brachydactyly type E (**Figure 2a,e,f**). The CNV is dominant and segregates perfectly with the trait in this large family (**Supplementary Figure S3**). The deletion is located within the regulatory archipelago of the *HOXD* gene cluster, which is essential for limb development, and removes

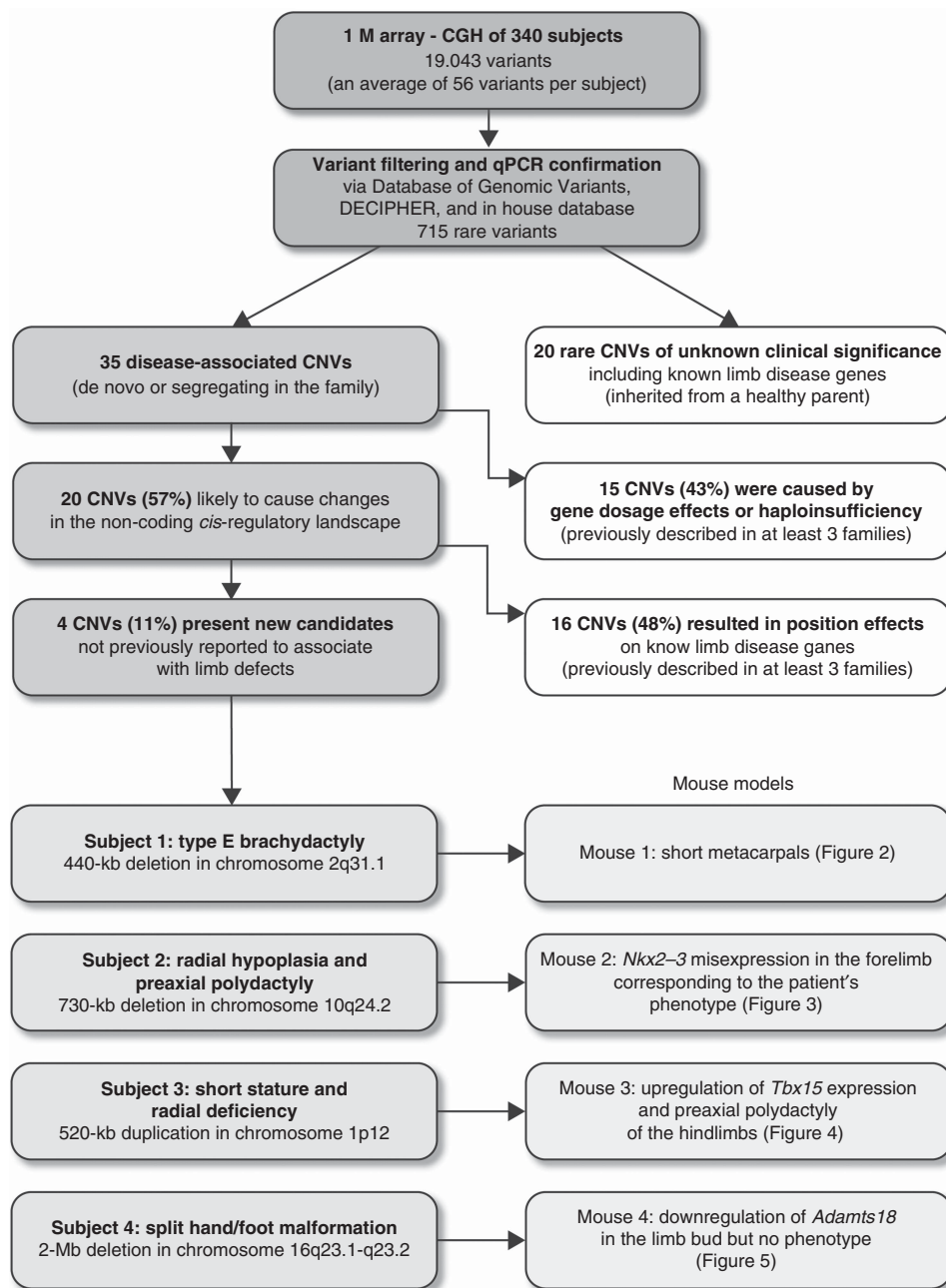


**Figure 1 Study design and workflow.** High-resolution array CGH was performed as a first screening test in a cohort of 340 individuals affected with isolated congenital limb malformations.

several known limb enhancer elements.<sup>18</sup> We bred homozygous *HoxD*<sup>Del(rel5-Atf2)</sup> mice harboring a similar deletion at the *Hoxd* cluster (Supplementary Figure S4). Montavon et al.<sup>18</sup> originally created this mouse model to characterize regulatory elements at the *HoxD* locus. We performed skeletal staining of homozygous *Del(rel5-Atf2)* embryos at E18.5 and identified severe shortening of the metacarpals, thus recapitulating the human brachydactyly phenotype (Figure 2f). In mice, the deletion results in a 90% reduction of *Hoxd13* expression—a known disease gene for brachydactyly type E.<sup>18</sup>

Subject 2 presented with preaxial polydactyly of the hands and proximal hypoplasia of the radius (Figure 3a). We detected a de novo 730-kb microdeletion on chromosome 10q24.2 (Figure 3b and Supplementary Figure S5), which removes three protein-coding genes with no established role in limb development.<sup>35</sup> Two known limb enhancers map centromeric to the deleted region<sup>24,29,36</sup> and the deletion also removes a TAD boundary (Figure 3b).<sup>31</sup> We suspected enhancer adoption and engineered mice with the corresponding deletion to investigate the expression of the telomeric gene *NKX2-3*.<sup>5</sup> Our data show that *Nkx2-3* was

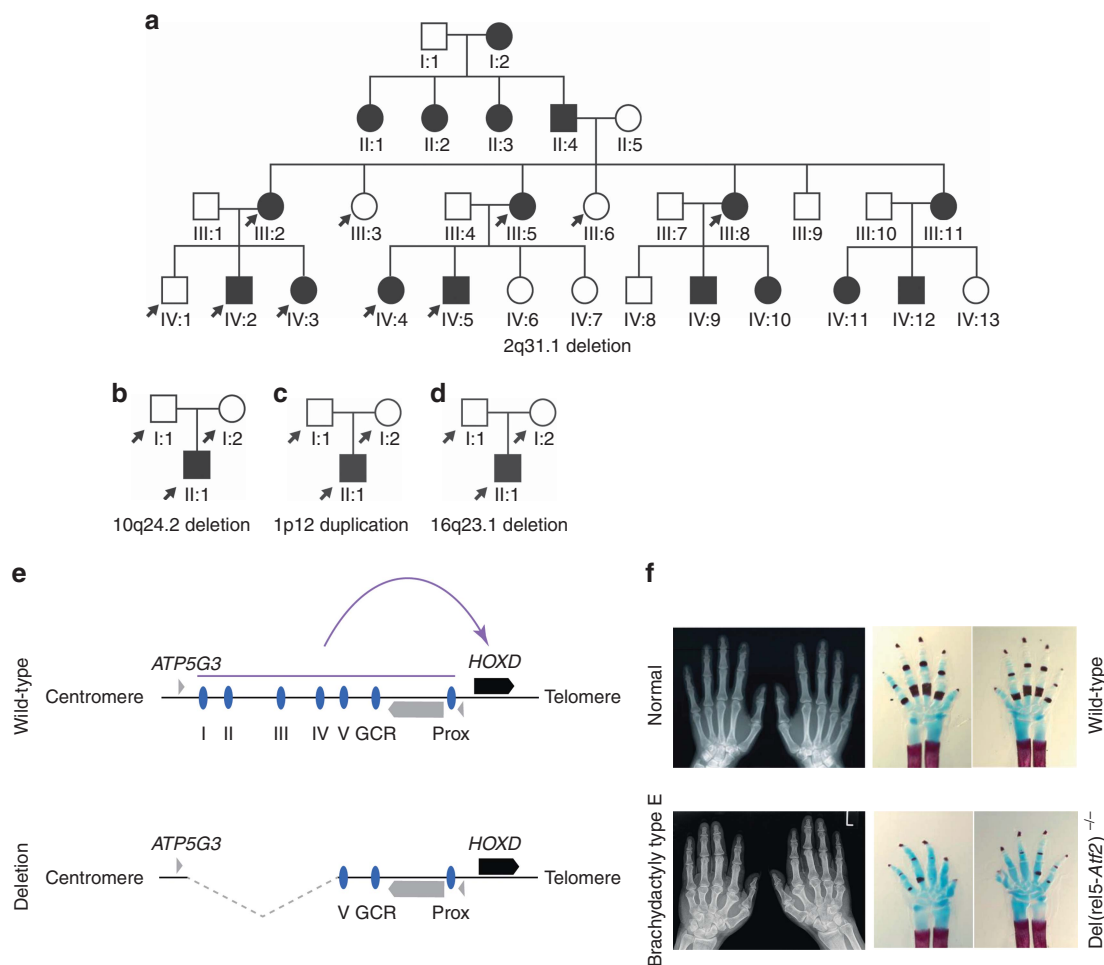


**Figure 2** CNVs detected in four unrelated families that were previously not known to be associated with limb malformations. (a–d) These candidate CNVs were either segregating with the phenotype (a) or true de novo in the index (b–d). The arrows indicate individuals tested for CNVs by array CGH or qPCR. Filled-in circles and squares represent individuals with clinical features and array CGH or qPCR abnormalities. (e) A 440-kb microdeletion on chromosome 2q31 was identified segregating in a large family affected with type E brachydactyly. The deletion is located within the regulatory archipelago of the *HOXD* gene cluster and removes several enhancer elements (blue ovals), thereby inducing a loss of *HOXD13* expression.<sup>18</sup> (f) Top: radiograph of a normal hand and a wild-type mouse paw (bones are stained in the metacarpals). Bottom: *Del(rel5-Atf2)* mice have an overlapping deletion as the patients at the *HoxD* cluster (Supplementary Figure S4).<sup>18</sup> Skeletal staining of homozygous *Del(rel5-Atf2)* mice embryos at E18.5 revealed reduced ossification and severe shortening of the metacarpals, thus resembling human brachydactyly type E. GCR, global control region; Prox, prox enhancer.

indeed misexpressed in the forelimb (Figure 3b), corresponding to the patient’s phenotype. However, we did not observe any limb abnormalities at E18.5. A larger control deletion including the limb enhancers showed no misexpression of *Nkx2–3* (Figure 3b). Our data suggest that enhancer adoption is the driver of ectopic *Nkx2–3* expression in the limb.

In subject 3, who was affected by short stature and radial deficiency, a de novo 520-kb microduplication on chromosome 1p12 was identified (Figure 4a,b and Supplementary Figure S6). The duplication is located centromeric to *TBX15*, a key gene in limb development, and encompasses the enhancer element *hs1428*,<sup>23</sup> which was shown to drive expression in the limb bud in a *Tbx5*-like fashion (Figure 4c,d). Mice with the corresponding duplication showed an upregulation of *Tbx15* expression at E11.5 (Figure 4e). In contrast to the patient’s phenotype, mice with the deletion showed preaxial polydactyly

of the hindlimbs (Figure 4f), indicating that the deletion has an effect on limb development, albeit with a different outcome in mice compared with humans.

In subject 4, presenting with split hand/foot malformation, a de novo 2-Mb deletion on chromosome 16q23.1–q23.3 was detected (Figure 5a and Supplementary Figure S7). The deletion removes four protein-coding genes without any established role in limb development<sup>35</sup> for which several loss-of-function mutations have been described in the Exome Aggregation Consortium database. The deletion also removes two TAD boundary elements and several potential limb enhancer elements marked by the histone modification H3K27ac in human embryonic limbs (Figure 5a).<sup>10,24</sup> We show that the flanking gene *Adamts18* is expressed in the apical ectodermal ridge of the developing mouse limb bud at E11.5 (Figure 5b). Mice harboring a human-like deletion

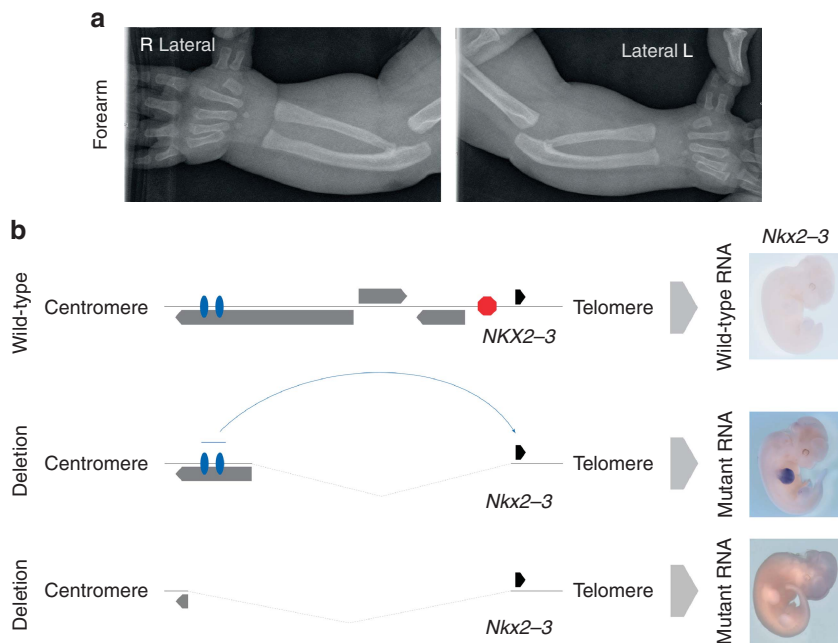


**Figure 3** Enhancer adoption at the *NKX2-3* locus is associated with radial hypoplasia and preaxial polydactyly in humans and resulted in gene misexpression in mice. (a) Radiographs of the forearms of subject 2, who is affected with proximal radial hypoplasia, radio-ulnar synostosis, and preaxial polydactyly. L, left; R, Lat, lateral; right. (b) Copy-number analysis revealed a de novo 730-kb microdeletion on chromosome 10q24.2. The deletion removes three protein-coding genes with no known role in limb development and a TAD boundary (indicated by the red octamer). Without the boundary, two known limb enhancers (blue ovals)<sup>24,29,36</sup> are free to act on the gene telomeric to the *NKX2-3* deletion. Mice with the corresponding deletion showed misexpression of *Nkx2-3* in the forelimb at E11.5 compared with wild-type mice. A larger control deletion including the limb enhancers showed no misexpression of *Nkx2-3* in the limb bud.

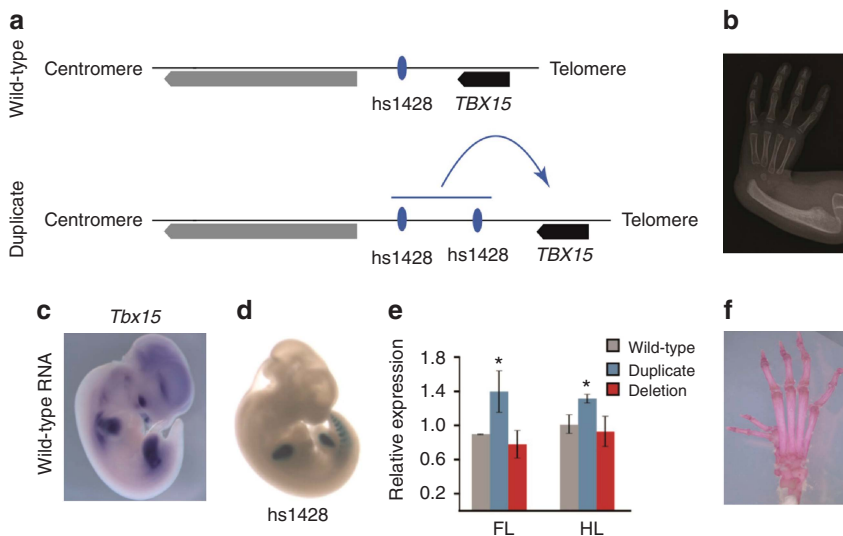


**Figure 4** Duplication of an enhancer element close to *TBX15* is associated with radial ray deficiency. (a) A de novo 520-kb microduplication on chromosome 1p12 was detected in subject 3, who was affected with short stature, radial deficiency, and thumb aplasia. The duplication is located centromeric to the transcription factor *TBX15*, a key gene in limb development, and encompasses the known limb enhancer element *hs1428* (blue ovals).<sup>23</sup> (b) A radiograph showing radial deficiency and thumb aplasia in subject 3. (c) Endogenous expression of *Tbx15*. (d) Enhancer-induced reporter gene expression in a LacZ reporter assay, closely resembling (c) and leading to the hypothesis that the duplication of *hs1428* might result in misexpression of *TBX15* in the developing limb, thereby contributing to the radial ray deficiency. (e) Mice with the corresponding duplication showed an upregulation of *Tbx15* expression at E11.5. (f) Preaxial polydactyly of the hindlimbs in a mouse with the corresponding duplication. FL, forelimb; HL, hindlimb. \**P*-value <0.05. Error bars: STD.

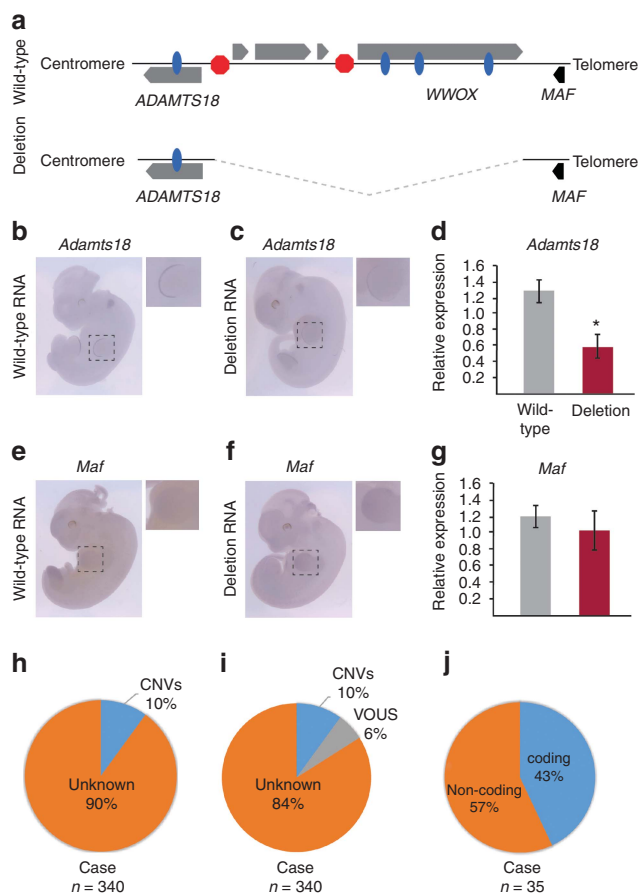


**Figure 5 A de novo 2-Mb deletion on chromosome 16q23.1-q23.3 in a patient with split hand/foot malformation.** (a) In subject 4, who presented with split hand/foot malformation, a de novo 2-Mb deletion on chromosome 16q23.1-q23.3 was detected. The deletion removes four protein-coding genes without any established role in limb development.<sup>35</sup> The deletion also removes two TAD boundary elements (red) and several potential limb enhancer elements marked by the histone modification H3K27ac in human embryonic limbs (blue ovals).<sup>10,24</sup> (b) The flanking gene *Adamts18* is expressed in the apical ectodermal ridge of the developing mouse limb bud at E11.5. (c) Mice harboring a human-like deletion do not show ectopic expression of *Adamts18*. (d) Mice harboring a human-like deletion show significant downregulation of *Adamts18* in the limb. \* $P < 0.05$ . (e) The gene located telomeric to the deletion *Maf* is also expressed in the developing mouse limb bud at E11.5. (f,g) Mice harboring a human-like deletion are phenotypically normal at birth (f) and show no altered expression of *Maf* in the limb (g). (h) A total of 35 disease-associated CNVs (true de novo or segregating in the family) were identified in a cohort of 340 unrelated individuals with congenital limb malformations, corresponding to an overall CNV rate of 10%. (i) Of the 340 subjects, 20 (6%) carried rare CNVs of unknown clinical significance (VOUS) that were inherited from a healthy parent. (j) Only 43% (15 cases) of the disease-associated CNVs included a known limb gene causing gene dosage effects or haploinsufficiency, whereas most of the CNVs (57%) were likely to cause changes in the noncoding *cis*-regulatory landscape. Error bars: STD.

showed significant downregulation of *Adamts18* in the limb ( $P < 0.05$ ) (Figure 5c,d). The gene located telomeric to the deletion *Maf* also showed expression during limb development at E11.5 (Figure 5e,f), but mice harboring a human-like deletion showed no altered expression of *Maf* in the limb (Figure 5g); in particular, *Maf* did not adopt *Adamts18*-like expression in the apical ectodermal ridge. All mice harboring the homozygous deletion were phenotypically normal at birth. *Adamts18* knockout mice do not show a limb phenotype,<sup>37</sup> indicating that the downregulation of *Adamts18* is not the underlying disease mechanism or that mouse and humans respond differently to the observed deletion.

Together, these results provide evidence for disease association of the first three CNVs (subjects 1–3) by regulatory loss of function, enhancer adoption, and regulatory

gain of function, respectively. However, it remains unclear if the de novo deletion in subject 4 is causative for the split hand/foot phenotype.

### Very rare inherited CNVs

In 20 of the 340 subjects (6%), we identified very rare CNVs of unknown clinical significance that were inherited from a healthy parent (Figure 5i). These rare CNVs involved important limb genes (e.g., *FGFR2*, *GNAS*, *GREM1*, and *RUNX2*) and were likely to play a role in the skeletal phenotypes, since a reduced penetrance is often present in limb malformations.<sup>1</sup> However, it needs to be considered that these rare inherited CNVs may not have been responsible for the limb defects. The clinical descriptions and family histories of the subjects can be found in Supplementary Table S5.

### Most CNVs in congenital limb malformation affect noncoding regulatory elements

In this study, we identified 35 disease-associated CNVs (de novo or segregating with the phenotype) in a cohort of 340 individuals with congenital limb malformations, which corresponds to 10% (Figure 5h,i and Supplementary Tables S1, 3, and 4). This is comparable to copy-number studies of intellectual disability, in which array CGH was the first-line test and usually 10–15% of the patients harbored de novo CNVs.<sup>16</sup> Interestingly, only 43% of the CNVs identified here directly included a known limb gene causing gene dosage effects or haploinsufficiency (Figure 5i,j and Supplementary Table S3), whereas most of the CNVs (57%) were localized in noncoding regions. Of those cases, 46% (16 cases) resulted in position effects on known limb disease genes that had previously been described in at least three unrelated families (Figure 5j and Supplementary Table S4). The remaining 11% (four cases) present new candidate CNVs not previously reported to be associated with limb defects.

### DISCUSSION

In this study, we applied high-resolution copy-number analysis to 340 unrelated subjects with congenital limb malformation and identified disease-associated CNVs in 10% of the cases studied, which is comparable to copy-number studies in other cohorts, such as in individuals affected with intellectual disability.<sup>16</sup> To investigate the four candidate CNVs not previously reported to associate with limb malformations, we generated mouse models. Our results indicate that CNVs have the potential to interfere with normal gene regulation by either altering enhancer dosage or changing the TAD architecture of the genome. Deletions that remove TAD boundaries can result in gene misexpression and consecutive disease. In our cohort, most of the CNVs (57%) affected the noncoding *cis*-regulatory genome, while only 43% included a known disease gene and therefore likely result in gene dosage effects. Our findings suggest that CNVs affecting noncoding regulatory elements are a major cause of congenital limb malformations.

Our data have several implications for the clinical interpretation of CNVs. First, we show that the proportion of CNVs that cause position effects is much higher than previously expected, at least in limb malformations.<sup>38,39</sup> While only two CNVs reported here do not include a gene at all (and are therefore truly noncoding), most of the CNVs include genes that are not involved in limb development. Our data indicate that CNVs can also alter genomic architecture by deleting or duplicating enhancer elements or misplacing TAD boundaries, thereby allowing enhancers from neighboring domains to ectopically activate genes, resulting in misexpression and disease. Several recent studies have also highlighted the role of rare noncoding variants as risk factors for autism spectrum disorder.<sup>40,41</sup> These mutational mechanisms must be considered when medically interpreting CNVs.<sup>3,13,14</sup>

Second, our study represents the largest CNV screen in patients with isolated congenital limb malformation so far. Similar large-scale CNV morbidity maps already exist for

developmental delay<sup>16</sup> and congenital kidney malformation<sup>42</sup> and have proven to be important resources for the clinical interpretation of CNVs. We identified 715 CNVs in 340 individuals that are either extremely rare or have not previously been reported in the common databases such as DECIPHER, ClinVar, and the Database of Genomic Variants (Supplementary Information). We show that 35 of these CNVs are de novo or segregate with the phenotype in the family, while 20 were inherited from a healthy parent and represent variants of unknown clinical significance. This unique CNV map represents a powerful resource for the study of limb malformations, in particular since reduced penetrance is a key feature in limb defects.<sup>1</sup>

Our study also has several limitations. First, not all human candidate CNVs result in a similar phenotype in mice. Therefore, defining the clinical relevance of these CNVs remains difficult. While we observed a human-like phenotype for the re-engineered deletion at the *HOXD* locus, others resulted only in a molecular phenotype or a different limb phenotype. The inheritance patterns of the CNVs and our functional data provide evidence for the disease association of the first three CNVs (subjects 1–3). However, it remains unclear if the de novo deletion in subject 4 was causative for the split hand/foot phenotype. For further validation of the candidate CNVs, more unrelated families must be identified. Our data also demonstrate the limitations of mouse models of human congenital disease. The differences between human and mouse phenotypes are most likely a result of species differences, as well as enhancer redundancy in mice, which has been described in several recent studies.<sup>3,43</sup>

Second, the CNV detection rate of 10% in patients with congenital limb malformation reported here might be slightly overestimated since our cohort is partially biased by the initial clinical selection. In this study, array CGH was used as a first screening test for all samples, but some samples were sent to us by collaborating laboratories only after candidate gene testing was performed and yielded no result. Third, our cohort is enriched with split hand/foot patients for whom chromosomal rearrangements are the more frequent cause.

An important question is whether our results are specific to limb malformations and to what extent noncoding CNVs affect other cohorts (e.g., intellectual disability). In many cohorts, CNVs are exclusively interpreted by the gene dosage approach,<sup>16,42</sup> and future studies must account for the *cis*-regulatory landscape of CNVs when attempting to identify potential target genes.

### SUPPLEMENTARY MATERIAL

Supplementary material is linked to the online version of the paper at <http://www.nature.com/gim>

### ACKNOWLEDGMENTS

We thank the families for their collaboration and contribution to this project, as well as Fabienne Pritsch, Judith Fiedler, and Karol Macura for technical support. We thank Sylvie Marx and Sean



Nader for providing clinical information and patient samples. This work was supported by a grant from the Deutsche Forschungsgemeinschaft to S.M. M.S. was supported by a grant from the Deutsche Forschungsgemeinschaft (SP1532/2-1) and by a fellowship of the Berlin-Brandenburg School for Regenerative Therapies. A.J. was supported by Polish National Science Centre grants (UMO-2011/03/B/NZ5/00510, 2011/03/D/NZ2/06136 and UMO-2016/22/E/NZ5/00270) as well as by the Polish National Centre for Research and Development (grant LIDER/008/431/L-4/12/NCBR/2013). A.S.-S. was supported by the Polish National Science Centre scholarship for PhD students (UMO-2013/08/T/NZ2/00027).

## DISCLOSURE

The authors declare no conflict of interest.

## REFERENCES

- Albers CA, Paul DS, Schulze H, et al. Compound inheritance of a low-frequency regulatory SNP and a rare null mutation in exon-junction complex subunit RBM8A causes TAR syndrome. *Nat Genet* 2012;44:435–439.
- Petit F, Sears KE, Ahituv N. Limb development: a paradigm of gene regulation. *Nat Rev Genet* 2017;18:245–258.
- Lupianez DG, Kraft K, Heinrich V, et al. Disruptions of topological chromatin domains cause pathogenic rewiring of gene-enhancer interactions. *Cell* 2015;161:1012–1025.
- Spielmann M, Brancati F, Krawitz PM, et al. Homeotic arm-to-leg transformation associated with genomic rearrangements at the PITX1 locus. *Am J Hum Genet* 2012;91:629–635.
- Spielmann M, Mundlos S. Structural variations, the regulatory landscape of the genome and their alteration in human disease. *Bioessays* 2013;35:533–543.
- Dathe K, Kjaer KW, Brehm A, et al. Duplications involving a conserved regulatory element downstream of *BMP2* are associated with brachydactyly type A2. *Am J Hum Genet* 2009;84:483–492.
- Franke M, Ibrahim DM, Andrey G, et al. Formation of new chromatin domains determines pathogenicity of genomic duplications. *Nature* 2016;538:265–269.
- Benko S, Gordon CT, Mallet D, et al. Disruption of a long distance regulatory region upstream of *SOX9* in isolated disorders of sex development. *J Med Genet* 2011;48:825–830.
- Fernandez BA, Siegel-Bartelt J, Herbrick JA, Teshima I, Scherer SW. Holoprosencephaly and cleidocranial dysplasia in a patient due to two position-effect mutations: case report and review of the literature. *Clin Genet* 2005;68:349–359.
- Dixon JR, Selvaraj S, Yue F, et al. Topological domains in mammalian genomes identified by analysis of chromatin interactions. *Nature* 2012;485:376–380.
- Lieberman-Aiden E, van Berkum NL, Williams L, et al. Comprehensive mapping of long-range interactions reveals folding principles of the human genome. *Science* 2009;326:289–293.
- Van Bortle K, Nichols MH, Li L, et al. Insulator function and topological domain border strength scale with architectural protein occupancy. *Genome Biol* 2014;15:R82
- Hnisz D, Weintraub AS, Day DS, et al. Activation of proto-oncogenes by disruption of chromosome neighborhoods. *Science* 2016;351:1454–1458.
- Lupianez DG, Spielmann M, Mundlos S. Breaking TADs: how alterations of chromatin domains result in disease. *Trends Genet* 2016;32:225–237.
- Gillissen C, Hehir-Kwa JY, Thung DT, et al. Genome sequencing identifies major causes of severe intellectual disability. *Nature* 2014;511:344–347.
- Cooper GM, Coe BP, Girirajan S, et al. A copy number variation morbidity map of developmental delay. *Nat Genet* 2011;43:838–846.
- Kraft K, Geuer S, Will AJ, et al. Deletions, inversions, duplications: engineering of structural variants using CRISPR/Cas in mice. *Cell Rep* 2015; e-pub ahead of print 4 February 2015.
- Montavon T, Soshnikova N, Mascrez B, et al. A regulatory archipelago controls *Hox* genes transcription in digits. *Cell* 2011;147:1132–1145.
- Artus J, Hadjantonakis AK. Generation of chimeras by aggregation of embryonic stem cells with diploid or tetraploid mouse embryos. *Methods Mol Biol* 2011;693:37–56.
- Albrecht AN, Schwabe GC, Stricker S, Boddlich A, Wanker EE, Mundlos S. The synpolydactyly homolog (*spdh*) mutation in the mouse —a defect in patterning and growth of limb cartilage elements. *Mech Dev* 2002;112:53–67.
- Firth HV, Richards SM, Bevan AP, et al. DECIPHER: database of chromosomal imbalance and phenotype in humans using ensembl resources. *Am J Hum Genet* 2009;84:524–533.
- Landrum MJ, Lee JM, Riley GR, et al. ClinVar: public archive of relationships among sequence variation and human phenotype. *Nucleic Acids Res* 2014;42:D980–D985.
- Visel A, Minovitsky S, Dubchak I, Pennacchio LA. VISTA Enhancer Browser —a database of tissue-specific human enhancers. *Nucleic Acids Res* 2007;35:D88–D92.
- Cotney J, Leng J, Yin J, et al. The evolution of lineage-specific regulatory activities in the human embryonic limb. *Cell* 2013;154:185–196.
- Kohler S, Doelken SC, Mungall CJ, et al. The Human Phenotype Ontology project: linking molecular biology and disease through phenotype data. *Nucleic Acids Res* 2014;42:D966–D974.
- Robinson PN, Kohler S, Oellrich A, et al. Improved exome prioritization of disease genes through cross-species phenotype comparison. *Genome Res* 2014;24:340–348.
- Eppig JT, Blake JA, Bult CJ, Kadin JA, Richardson JE, Mouse Genome Database Group. The Mouse Genome Database (MGD): facilitating mouse as a model for human biology and disease. *Nucleic Acids Res* 2015;43:D726–D736.
- Smith CM, Finger JH, Hayamizu TF, et al. GXD: a community resource of mouse gene expression data. *Mamm Genome* 2015;26:314–324.
- Visel A, Blow MJ, Li Z, et al. ChIP-seq accurately predicts tissue-specific activity of enhancers. *Nature* 2009;457:854–858.
- VanderMeer JE, Smith RP, Jones SL, Ahituv N. Genome-wide identification of signaling center enhancers in the developing limb. *Development* 2014;141:4194–4198.
- Rao SS, Huntley MH, Durand NC, et al. A 3D map of the human genome at kilobase resolution reveals principles of chromatin looping. *Cell* 2014;159:1665–1680.
- Klopocki E, Lohan S, Doelken SC, et al. Duplications of *BHLHA9* are associated with ectrodactyly and tibia hemimelia inherited in non-Mendelian fashion. *J Med Genet* 2012;49:119–125.
- Malik S, Percin FE, Bornholdt D, et al. Mutations affecting the BHLHA9 DNA-binding domain cause MSSD, mesoaxial synostotic syndactyly with phalangeal reduction, Malik–Percin type. *Am J Hum Genet* 2014;95:649–659.
- Nevado J, Mergener R, Palomares-Bralo M, et al. New microdeletion and microduplication syndromes: a comprehensive review. *Genet Mol Biol* 2014;37:210–219.
- Eppig JT, Motenko H, Richardson JE, Richards-Smith B, Smith CL. The International Mouse Strain Resource (IMSR): cataloging worldwide mouse and ES cell line resources. *Mamm Genome* 2015;26:448–455.
- Symmons O, Uslu VV, Tsujimura T, et al. Functional and topological characteristics of mammalian regulatory domains. *Genome Res* 2014;24:390–400.
- Dickinson ME, Flenniken AM, Ji X, et al. High-throughput discovery of novel developmental phenotypes. *Nature* 2016;537:508–514.
- Ibn-Salem J, Kohler S, Love MI, et al. Deletions of chromosomal regulatory boundaries are associated with congenital disease. *Genome Biol* 2014;15:423
- Kleinjan DJ, van Heyningen V. Position effect in human genetic disease. *Hum Mol Genet* 1998;7:1611–1618.
- Talkowski ME, Rosenfeld JA, Blumenthal I, et al. Sequencing chromosomal abnormalities reveals neurodevelopmental loci that confer risk across diagnostic boundaries. *Cell* 2012;149:525–537.
- Walker S, Scherer SW. Identification of candidate intergenic risk loci in autism spectrum disorder. *BMC Genomics* 2013;14:499
- Sanna-Cherchi S, Kiryluk K, Burgess KE, et al. Copy-number disorders are a common cause of congenital kidney malformations. *Am J Hum Genet* 2012;91:987–997.
- Spielmann M, Kakar N, Tayebi N, et al. Exome sequencing and CRISPR/Cas genome editing identify mutations of *ZAK* as a cause of limb defects in humans and mice. *Genome Res* 2016;26:183–191.